

Liquid–Liquid Equilibria for the Binary Systems of *N*-Formylmorpholine with Cycloalkanes

MinSu Ko,[†] Sangyoun Na,[†] Sungjin Lee,[‡] and Hwayong Kim^{*†}

School of Chemical Engineering & Institute of Chemical Processes, Seoul National University, Shinlim-dong, Kwanak-gu, Seoul 151-744, Korea; and School of General Education, Semyung University, Sinwol-dong, Jechon, Chungbuk 390-711, Korea

Liquid–liquid equilibrium (LLE) data were measured for three binary systems containing *N*-formylmorpholine and cycloalkanes (cyclopentane, cyclohexane, and cyclooctane) over the temperature a circulation type instrument with an equilibrium view cell. The compositions of both cycloalkane-rich and *N*-formylmorpholine-rich phases were analyzed by on-line gas chromatography. The binary liquid–liquid equilibrium data were correlated with the NRTL and UNIQUAC equations using temperature-dependent parameters. The NRTL and UNIQUAC equations fitted the experimental data of the equilibria with a good precision, although a clear deviation was observed in the vicinity of the upper critical solution temperature (UCST). The properties for the critical point are expressed in terms of an exponential law. The solubility of cycloalkanes in the *N*-formylmorpholine increases in the following order at the same temperature: cyclopentane, cyclohexane, and cyclooctane.

Introduction

The *N*-formylmorpholine (NFM) extractive distillation process separates aromatics from the reformates¹ at the operating temperature ranging from 350 to 430 K. The design and operation of the extractive distillation column requires the quantitative information of the phase equilibria. The commercial process simulators such as Aspen Plus, Hysys, and Pro II have been used to optimize the operating conditions. However, the thermodynamic properties data of *N*-formylmorpholine are not built in the commercial simulators, and the liquid–liquid equilibria data are also scarce for the binary systems containing *N*-formylmorpholine in the literature (*n*-alkanes + NFM^{2,3,18} and isoalkanes + NFM³). To our knowledge, the liquid–liquid equilibria on cycloalkane and *N*-formylmorpholine systems have not been published.

The liquid–liquid equilibria for the *N*-formylmorpholine and cycloalkane (cyclopentane, cyclohexane, and cyclooctane) binary systems were measured at the temperature range from about 300 K to the vicinity of the upper critical solution temperature (UCST), and the compositions at the critical point are estimated with an exponential law.^{4–16,19–26} Experimental data were correlated with the nonrandom two-liquid (NRTL)¹⁶ and universal quasi-chemical (UNIQUAC)¹⁷ models with the temperature-dependent parameters.¹⁸

Experimental Section

Chemicals. The suppliers and purities of the chemicals are listed in Table 1 together with the purities determined using a HP 5890 gas chromatograph with a thermal conductivity detector. The chemicals were used without purification.

* To whom correspondence should be addressed. Fax: +82-2-888-6695. E-mail: hwayongk@snu.ac.kr.

[†] Seoul National University.

[‡] Semyung University.

Table 1. Suppliers and Purity of the Used Chemicals

chemical	supplier	spec ^a /%	purity ^b /%
NFM	ACROS	>99.00	>99.99
cyclopentane	ACROS	>99.00	>99.93
cyclohexane	Kanto Chemical Co., Inc.	>99.50	>99.93
cyclooctane	Tokyo Kasei Kogyo Co., Ltd.	>99.96	>99.95

^a The purity reported by the supplier. ^b The purity determined as an area ratio by the gas chromatography with a thermal conductivity detector.

Experimental Apparatus. Details of this apparatus are given in our previous studies.¹⁸ The volume of the equilibrium cell was 240 cm³. The cell was made of stainless steel (SUS. 316) and placed inside the air bath, controlled by a PID temperature controller to the desired temperature within ± 0.1 K (maximum temperature 573.2 K). The cell and the quartz window were sealed with PTFE (Teflon) gaskets. The mixing was promoted by the magnetic stirrer. The temperature was measured using a platinum resistance thermometer (1502A by Hart Scientific, Inc.). Its uncertainty was estimated to be within ± 0.006 K. The thermometer was calibrated at the ice point and by comparison to standard platinum thermometers (SPRTs) calibrated on the basis of the international temperature scale of 1990 (ITS-90). The sampling system was connected to a gas chromatograph (Hewlett-Packard 5890 series II) with a thermal conductivity detector (TCD) and a 1.828 m \times 0.003 175 m column packed with Chromosorb WHP 100/120 coated with OV-101.

Experimental Procedure. The mixture was fed into the equilibrium cell that was initially evacuated. The mixture was stirred for at least 1 h with the magnetic stirrer and then left to settle for at least 2 h. Each phase was circulated with recirculation pumps for 1 h. The sampling was performed when the cell temperature change was within ± 0.02 K for 10 min. The samples were analyzed by gas chromatography. The temperatures of the injector and the detector were maintained at 523.15 K. After 1 min of

Table 2. Experimental and Calculated LLE Data for the Cyclopentane (1) + *N*-Formylmorpholine (2) System

<i>T</i> /K	top phase, x_{11}			bottom phase, x_{12}		
	exp	NRTL	UNIQUAC	exp	NRTL	UNIQUAC
304.31	0.9833	0.9841	0.9841	0.1286	0.1253	0.1251
310.80	0.9828	0.9815	0.9815	0.1354	0.1357	0.1357
320.72	0.9745	0.9764	0.9764	0.1500	0.1554	0.1557
330.41	0.9721	0.9696	0.9697	0.1767	0.1803	0.1806
340.50	0.9614	0.9600	0.9600	0.2117	0.2138	0.2140
350.15	0.9438	0.9467	0.9467	0.2647	0.2558	0.2558
354.82	0.9351	0.9381	0.9381	0.2834	0.2808	0.2806
359.64	0.9257	0.9272	0.9272	0.3148	0.3107	0.3104
364.75	0.9142	0.9123	0.9123	0.3581	0.3480	0.3478
369.78	0.8953	0.8928	0.8928	0.3958	0.3927	0.3922
374.11	0.8704	0.8697	0.8696	0.4365	0.4398	0.4396
376.49	0.8575	0.8529	0.8529	0.4552	0.4708	0.4709
379.39	0.8227	0.8260	0.8260	0.5099	0.5168	0.5171
380.35	0.8121	0.8142	0.8143	0.5403	0.5340	0.5346

Table 3. Experimental and Calculated LLE Data for the Cyclohexane (1) + *N*-Formylmorpholine (2) System

<i>T</i> /K	top phase, x_{11}			bottom phase, x_{12}		
	exp	NRTL	UNIQUAC	exp	NRTL	UNIQUAC
303.05	0.9868	0.9868	0.9866	0.0776	0.0815	0.0793
308.15	0.9867	0.9848	0.9848	0.0824	0.0847	0.0836
313.04	0.9830	0.9827	0.9828	0.0919	0.0886	0.0883
322.78	0.9738	0.9776	0.9778	0.1019	0.0985	0.0996
333.24	0.9675	0.9704	0.9707	0.1203	0.1130	0.1153
342.89	0.9601	0.9615	0.9619	0.1360	0.1313	0.1343
353.64	0.9478	0.9477	0.9481	0.1567	0.1591	0.1623
363.42	0.9346	0.9299	0.9300	0.1863	0.1941	0.1969
373.06	0.9129	0.9041	0.9037	0.2315	0.2425	0.2437
382.42	0.8809	0.8645	0.8635	0.2961	0.3111	0.3092
389.83	0.8169	0.8111	0.8099	0.3836	0.3937	0.3876
391.57	0.7793	0.7927	0.7917	0.4448	0.4202	0.4132
391.62	0.7656	0.7921	0.7911	0.4289	0.4210	0.4139

holding at 353.15 K, the column temperature was raised to the final temperature of 423.15 K at the rate 25 K·min⁻¹. Helium was used as the carrier gas at the rate 23 cm³·min⁻¹. Single-phase samples of known composition were used to calibrate the gas chromatograph in the composition range of interest. The samples of each phase at the same temperature were analyzed at least three times, and the average values were used. The liquid-phase compositions were determined with a maximum relative error of 0.1%.

Results and Discussion

The measurements for the three systems cyclopentane (1) + *N*-formylmorpholine (2), cyclohexane (1) + *N*-formylmorpholine (2), and cyclooctane (1) + *N*-formylmorpholine (2) were performed over the temperature range from about 300 K to the vicinity of the upper critical solution temperature (UCST). The experimental data are given in Tables 2–4. The upper critical solution temperature was only observed and listed in Table 5. In the vicinity of the critical point, the corresponding thermodynamic functions, for example, $G(T, P, x)$, are not analytical because of the flat slopes of the two branches of the coexistence curve near the critical region. The theoretical approach to clarifying the critical phenomena led to the renormalization group (RG) theory.^{7,13–16,19–26} The RG theory is used to express the composition for the critical point. For a partially miscible binary liquid system, the coexistence curve describes the temperature dependence of the concentration range over which the two components are immiscible. The corresponding exponent β is defined through the relation¹⁹

$$\Delta M = B(\tau)^\beta \quad (1)$$

Table 4. Experimental and Calculated LLE Data for the Cyclooctane (1) + *N*-Formylmorpholine (2) System

<i>T</i> /K	top phase, x_{11}			bottom phase, x_{12}		
	exp	NRTL	UNIQUAC	exp	NRTL	UNIQUAC
301.99	0.9773	0.9749	0.9750	0.0514	0.0532	0.0528
310.99	0.9738	0.9738	0.9740	0.0542	0.0561	0.0559
320.88	0.9689	0.9714	0.9715	0.0625	0.0612	0.0611
330.36	0.9662	0.9676	0.9677	0.0724	0.0682	0.0684
340.50	0.9576	0.9616	0.9615	0.0848	0.0788	0.0792
349.95	0.9514	0.9532	0.9530	0.0954	0.0926	0.0933
359.24	0.9405	0.9410	0.9405	0.1108	0.1116	0.1125
368.31	0.9264	0.9231	0.9224	0.1326	0.1379	0.1390
373.27	0.9128	0.9094	0.9086	0.1568	0.1572	0.1583
378.04	0.9012	0.8922	0.8914	0.1761	0.1806	0.1814
382.71	0.8812	0.8700	0.8693	0.2010	0.2099	0.2103
387.68	0.8532	0.8370	0.8370	0.2360	0.2517	0.2508
389.37	0.8396	0.8224	0.8230	0.2438	0.2694	0.2680
390.27	0.8253	0.8138	0.8148	0.2626	0.2798	0.2780
391.70	0.8026	0.7984	0.8001	0.2872	0.2982	0.2956
392.16	0.6893	0.7929	0.7950	0.4025	0.3045	0.3017

Table 5. Calculated Data for the Upper Critical Solution Temperature and the Critical Mole Fraction

		T_c /K	x_c
cyclopentane (1) + <i>N</i> -formylmorpholine (2)	RG	381.145 ^a	0.673
	NRTL	384.786	0.690
	UNIQUAC	384.815	0.690
cyclohexane (1) + <i>N</i> -formylmorpholine (2)	RG	392.047 ^a	0.606
	NRTL	399.459	0.623
	UNIQUAC	399.262	0.616
cyclooctane (1) + <i>N</i> -formylmorpholine (2)	RG	392.407 ^a	0.547
	NRTL	400.406	0.560
	UNIQUAC	400.363	0.558

^a The upper critical solution temperature observed by the experimental apparatus.

where ΔM is the difference in order parameter between the coexisting phases. The current theoretical value of β is 0.325 ± 0.01 by the RG calculations^{20,21} and 0.312 ± 0.05 by the high-temperature series expansions.²² In the non-asymptotic region, eq 1 is modified by the presence of corrections to scaling.²³ When applied to fluids, this is of the form⁸

$$x_{11} - x_{12} = B_0 \tau^\beta [1 + B_1 \tau^{\Delta_1} + B_2 \tau^{2\Delta_1} + \dots] \quad (2)$$

where $\Delta_1 = 0.5$ is the correction exponent. It is of greater significance to the actual description of liquid–liquid-phase equilibria. It has become customary to use $\Delta_1 = 0.5$ as a fixed value while fitting the experimental data.^{7,24–26} $\tau = |T - T_c|/T_c$ is the reduced temperature and expresses the distance from the critical point. The value of the critical exponent, β , using eqs 2–4, is 0.325.¹⁶ The diameter of coexisting curves is given by the relationship⁸

$$(x_{11} + x_{12})/2 = x_c [1 + A_1 \tau + A_2 \tau^{1-\alpha} + \dots] \quad (3)$$

where α is the same critical exponent corresponding to the heat capacity.

Equations 2 and 3 are combined to give

$$x = x_c [1 + A_1 \tau + A_2 \tau^{1-\alpha} + \dots] + f B_0 \tau^\beta [1 + B_1 \tau^{\Delta_1} + B_2 \tau^{2\Delta_1} + \dots] \quad (4)$$

This relationship can be used to correlate the mutual solubility in a broader temperature interval, including the critical region ($f = 1$ for $x > x_c$ and $f = -1$ for $x < x_c$). Table 5 shows the values of the critical mole fraction calculated by the RG theory and the NRTL and UNIQUAC models.

Table 6. Coefficients in Eqs 2 and 3 by Fitting of the Experimental Data Given in Tables 2–4 for Cycloalkanes (1) + *N*-Formylmorpholine (2) Mixtures

	A_1	A_2	B_0	B_1	B_2	α
cyclopentane (1) + <i>N</i> -formylmorpholine (2)	-1.455	5.261	1.805	-0.699	0.631	-1.360
cyclohexane (1) + <i>N</i> -formylmorpholine (2)	-3.568	3.787	2.802	-1.939	2.017	-0.148
cyclooctane (1) + <i>N</i> -formylmorpholine (2)	629.4	-629.4	3.515	-2.397	2.557	0.0002

Table 7. Temperature Dependence of the Parameters of the NRTL Equation for the Cycloalkanes (1) + *N*-Formylmorpholine (2) Binary Systems^a

parameter	cyclopentane	cyclohexane	cyclooctane
a_{12}	52.256	20.719	233.71
a_{21}	102.84	120.47	165.34
b_{12}/K	-891.78	900.64	-10290.9
b_{21}/K	-3869.9	-4921.0	-7111.3
c_{12}	0.3	0.3	0.3
d_{12}/K^{-1}	0.0001	0.0001	0.0001
e_{12}	-8.027	-3.536	-34.457
e_{21}	-15.509	-17.927	-24.451

^a $c_{12} = c_{21}$; $d_{21}/K^{-1} = 0$.

Table 8. Temperature Dependence of the Parameters of the UNIQUAC Equation for the Cycloalkanes (1) + *N*-Formylmorpholine (2) Binary Systems

parameter	cyclopentane	cyclohexane	cyclooctane
a_{12}	-10.170	-6.647	-67.988
a_{21}	-28.838	-24.730	-17.232
b_{12}/K	56.438	-243.00	3052.5
b_{21}/K	1156.5	1091.9	683.49
c_{12}	1.570	1.110	9.954
c_{21}	4.329	3.661	2.603

The values of the critical mole fractions in cycloalkanes + *N*-formylmorpholine systems calculated from RG theory are smaller than those from the NRTL and UNIQUAC models. The coefficients, A_1 , A_2 , B_0 , B_1 , B_2 , and α , in eqs 2 and 3 are given in Table 6.

The binary liquid–liquid equilibrium data were correlated with the NRTL and UNIQUAC models using the following temperature-dependent binary parameters.

For the NRTL model

$$\tau_{ij} = a_{ij} + b_{ij}/T + e_{ij} \ln T \quad (5)$$

$$\alpha_{ij} = c_{ij} + d_{ij}(T - 273.15) \quad (6)$$

for the UNIQUAC model

$$\tau_{ij} = \exp(a_{ij} + b_{ij}/T + c_{ij} \ln T) \quad (7)$$

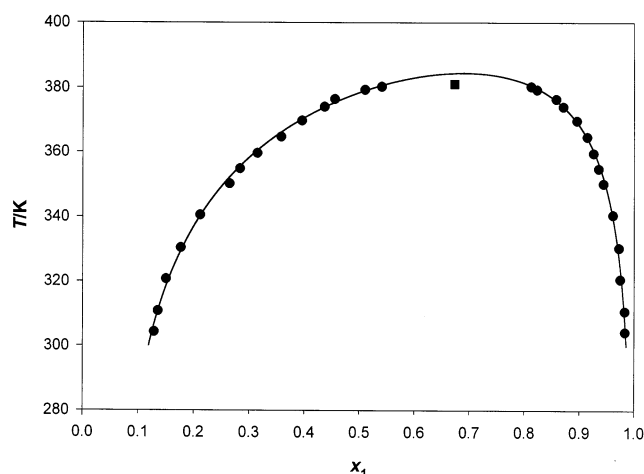
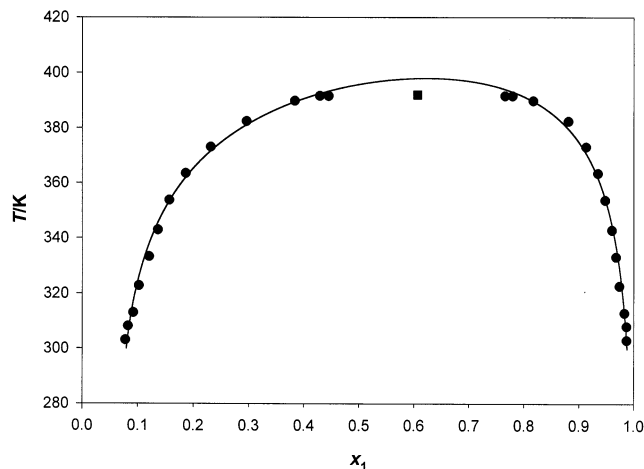
where T is the absolute temperature.

The temperature-dependent binary parameters are given in Tables 7 and 8. The binary parameters for the models were evaluated by a nonlinear regression method based on the maximum-likelihood. The objective function was minimized during optimization of the parameters in each of the equations:

$$OF = \sum_{k=1}^N \left\{ \left(\frac{T_k^{\text{cal}} - T_k^{\text{exp}}}{\sigma_{T_k}} \right)^2 + \sum_{i=1}^2 \sum_{j=1}^2 \left(\frac{x_{ij}^{\text{cal}} - x_{ij}^{\text{exp}}}{\sigma_{x_{ijk}}} \right)^2 \right\} \quad (8)$$

where N is the number of the experimental data in each group k and σ_k is the standard deviation of group k . The superscripts, cal and exp, present calculated property and experimental property, respectively.

Figures 1–3 show graphical representations of the experimental data and the calculated data in the form of T , x , x' diagrams, whereby the calculated values have been

**Figure 1.** Experimental and calculated liquid–liquid equilibrium data for the cyclopentane (1) + *N*-formylmorpholine (2) mixture: points, experimental results; black solid line, NRTL; square points (■), critical point calculated by eq 2.**Figure 2.** Experimental and calculated liquid–liquid equilibrium data for the cyclohexane (1) + *N*-formylmorpholine (2) mixture: points, experimental results; black solid line, NRTL; square points (■), critical point calculated by eq 2.

obtained by means of the NRTL equation. NRTL and UNIQUAC models in the vicinity of the critical temperature because of the nonanalytic behavior could not correlate the binary LLE data for the above-mentioned system. The NRTL and UNIQUAC models predict similar coexistence curves over a wide temperature range. The percent absolute average deviations (AAD%) of the NRTL and UNIQUAC equations are listed in Table 9. The NRTL model showed smaller deviations in both phases. The mutual solubility increases as the temperature increases for all these systems. The solubility of the cycloalkanes in *N*-formylmorpholine increased in the following order at the same temperature: cyclopentane, cyclohexane, and cyclooctane.

Conclusions

The interaction parameters of the NRTL and UNIQUAC equations have been determined for the *N*-formylmorpho-

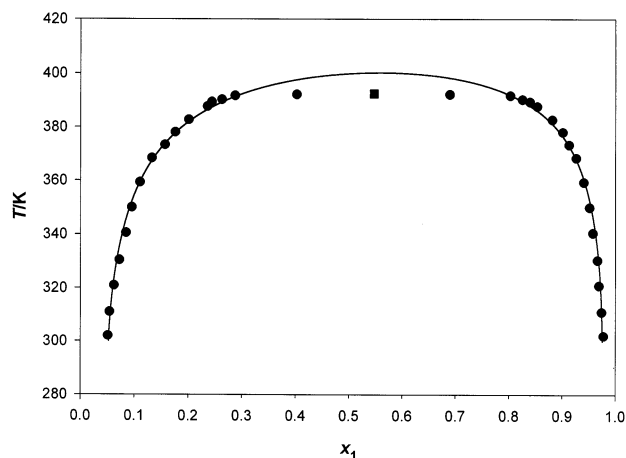


Figure 3. Experimental and calculated liquid–liquid equilibrium data for the cyclooctane (1) + *N*-formylmorpholine (2) mixture: points, experimental results; black solid line, NRTL; square points (■), critical point calculated by eq 2.

Table 9. Percent Absolute Average Deviations (AAD%)^a of the NRTL and UNIQUAC Equations for the Cycloalkanes (1) + *N*-Formylmorpholine (2) Binary Systems

system	x_{11}		x_{12}	
	NRTL	UNIQUAC	NRTL	UNIQUAC
cyclopentane + NFM	0.24	1.81	0.24	1.87
cyclohexane + NFM	0.79	3.83	0.80	3.53
cyclooctane + NFM	1.58	5.55	1.59	5.45

$$^a \text{AAD\%} = (1/N) \sum_{i=1}^N |(x_{1,\text{cal}} - x_{1,\text{exp}})/x_{1,\text{exp}}| \times 100.$$

line + cyclopentane, + cyclohexane, and + cyclooctane systems using the experimental data at 300 K to the UCST. The upper critical solution temperature and the critical mole fraction were determined using the exponential law. The temperature-dependent parameters of NRTL and UNIQUAC models can be expressed by eqs 5 and 7, respectively. Thus, a quantitative description of liquid–liquid equilibria of industrial interest containing *N*-formylmorpholine and cycloalkanes is available to accurately simulate and optimize the extractive distillation units where these systems are involved.

Literature Cited

- Morrison, S. G.; Brown, W. E. Reforming Process for Producing High Purity Benzene. *Zeolites* **1996**, *17*, 403.
- Mohamed, A. Q.; Taher, A. A.; Mohamed, A. F. Liquid–Liquid Equilibria in Some Binary and Ternary Mixtures with *N*-Formylmorpholine. *J. Chem. Eng. Data* **1995**, *40*, 88–90.
- Cincotti, A.; Murru, M.; Cao, G.; Marongiu, B.; Masia, F.; Sannia, M. Liquid–Liquid Equilibria of Hydrocarbons with *N*-Formylmorpholine. *J. Chem. Eng. Data* **1999**, *44*, 480–483.
- Rubio, M. A.; Gonzalez, J. A.; Garcia de la Fuente, I.; Cobos, J. C.; Thermodynamic Properties of *n*-Alkoxyethanols + Organic Solvent Mixtures. IX. Liquid–Liquid Equilibria of Systems Containing 2-Methoxyethanol or 2-Ethoxyethanol and Selected *n*-Alkanes. *J. Chem. Eng. Data* **1998**, *43*, 811–814.
- Hodges, D.; Pritchard, D. W.; Anwar, M. M. Liquid-liquid equilibria prediction using the area method. *Fluid Phase Equilib.* **1995**, *111*, 27–36.
- van't Hof, A.; Japas, L. M.; Peters, C. J. Description of liquid–liquid equilibria including the critical region with the crossover-NRTL model. *Fluid Phase Equilib.* **2001**, *192*, 27–48.
- Nagarajan, N.; Kumar, A.; Gopal, E. S. R.; Greer, S. C. Liquid–liquid critical phenomena. The coexistence curve of *n*-heptane-acetic anhydride. *J. Phys. Chem.* **1980**, *84*, 2883–2887.
- Ley-Koo, M.; Green, M. S. Revised and extended scaling for coexisting densities of SF₆. *Phys. Rev. A* **1977**, *16*, 2483–2487.
- Chen, Z. Y.; Abbaci, A.; Tang, S.; Sengers, J. V. Global thermodynamic behavior of fluids in the critical region. *Phys. Rev. A* **1990**, *42*, 4470–4484.
- Chen, Z. Y.; Albright, P. C.; Sengers, J. V. Crossover from singular critical to regular classical thermodynamic behavior of fluids. *Phys. Rev. A* **1990**, *41*, 3161–3177.
- Jin, G. X.; Tang, S.; Sengers, J. V. Global thermodynamic behavior of fluid mixtures in the critical region. *Phys. Rev. E* **1993**, *47*, 388–402.
- Nicoll, J. F. Critical phenomena of fluids: Asymmetric Landau-Ginzburg-Wilson model. *Phys. Rev. A* **1981**, *24*, 2203–2220.
- Nicoll, J. F.; Bhattacharjee, J. K. Crossover functions by renormalization-group matching: $O(\epsilon^2)$ results. *Phys. Rev. B* **1981**, *23*, 389–401.
- Nicoll, J. F.; Albright, P. C. Crossover functions by renormalization-group matching: Three-loop results. *Phys. Rev. B* **1985**, *31*, 4576–4589.
- Nicoll, J. F.; Albright, P. C. Crossover functions by renormalization-group matching: Three-loop results. *Phys. Rev. B* **1985**, *31*, 4576–4589.
- Kumar, A.; Krishnamurthy, H. R.; Gopal, E. S. R. Equilibrium Critical Phenomena in Binary Liquid Mixtures. *Phys. Rep.* **1983**, *2*, 57–143.
- Abrams, D. S.; Prausnitz, J. M. Statistical Thermodynamics of Liquid Mixtures; A New Expression for the Excess Gibbs Energy of Partly or Completely Miscible Systems. *AIChE J.* **1975**, *21*, 116–128.
- Ko, M.; Lee, S.; Cho, J.; Kim, H. Liquid-Liquid Equilibria for Binary Systems Containing *N*-Formylmorpholine. *J. Chem. Eng. Data* **2002**, *47*, 923–926.
- Levelt Sengers, J. M. H.; Greer, W. L.; Sengers, J. V. Scaled equation of state parameters for gases in the critical region. *J. Phys. Chem. Ref. Data* **1976**, *5*, 1–52.
- Le Guillou, J. C.; Zinn-Justin, J. Critical Exponents for the *n*-Vector Model in Three Dimensions from Field Theory. *Phys. Rev. Lett.* **1977**, *39*, 95–98.
- Le Guillou, J. C.; Zinn-Justin, J. Critical exponents from field theory. *Phys. Rev. B* **1980**, *21*, 3976–3998.
- Domb, C.; Green, M. S. *Phase Transition and Critical Phenomena*; Academic: New York, 1974; p 3.
- Wegner, F. J. Corrections to Scaling Laws. *Phys. Rev. B* **1972**, *5*, 4529–4536.
- Saul, D. M.; Wortis, M.; Jasnow, D. Confluent singularities and the correction-to-scaling exponent for the $d=3$ fcc Ising model. *Phys. Rev. B* **1975**, *11*, 2571–2578.
- Greer, S. C. Coexistence curves at liquid–liquid critical points: Ising exponents and extended scaling. *Phys. Rev. A* **1976**, *14*, 1770–1780.
- Nakata, M.; Dobashi, T.; Kuwahara, N.; Kaneko, M. Coexistence curve and diameter of polystyrene in cyclohexane. *Phys. Rev. A* **1978**, *18*, 2683–2688.

Received for review May 13, 2002. Accepted October 18, 2002. This work was supported by the Brain Korea 21 Program supported by the Ministry of Education and LG-Caltex Research and by the National Research Laboratory (NRL) Program supported by Korea Institute of S&T Evaluation and Planning.

JE020089J